Journal of Power Sources 199 (2012) 117–123

Contents lists available at SciVerse ScienceDirect

Journal of Power Sources

journal homepage: www.elsevier.com/locate/jpowsour

Design of thermal self supported 700 W class, solid oxide fuel cell module using, LSGM thin film micro tubular cells

Naoki Watanabe[a,c,*], Toshiharu Ooe[c], Tatsumi Ishihara[a,b]

[a] Department of Automotive Science, Graduate School of Integrated Frontier Sciences, Kyushu University, 744 Motooka, Nishi-ku, Fukuoka 819-0395, Japan
[b] Department of Applied Chemistry, Faculty of Engineering, Kyushu University, 744 Motooka, Nishi-ku, Fukuoka 819-0395, Japan
[c] TOTO LTD., 2-8-1 Honson, Chigasaki-City, Kanagawa 253-8577, Japan

ARTICLE INFO

Article history:
Received 31 May 2011
Received in revised form 23 August 2011
Accepted 18 October 2011
Available online 21 October 2011

Keywords:
Solid oxide fuel cell
Module design
Micro tubular design
Thermal self supported condition
$La_{0.8}Sr_{0.2}Ga_{0.8}Mg_{0.2}O_{2.8}$ electrolyte

ABSTRACT

Thermal self supporting SOFC module was studied under various conditions for high energy conversion efficiency. In order to achieve high energy conversion efficiency even under partial load condition, SOFC module and system was designed to operate at intermediate temperature by using $LaGaO_3$ based oxide film electrolyte. Heat loss, $Q_{heatloss}$ is requested to be diminished as much as possible by decreasing heat radiation and exhaust gas heat from module. SOFC module with 700 W was successfully demonstrated in thermal self-supported state under various conditions. SOFC module can be thermally self-supported within a limited temperature range (841–886 K) but energy conversion efficiency decreases with decreasing current density, because of the limited fuel and air utilization from heat value requested for thermal self-support. In this study, the energy conversion efficiency of the 700 W module shows ca. 47% low heat value (LHV) at 700 W output power with fuel utilization of 75% and even at 250 W partial load, efficiency is ca. 30% achieved. For achieving the high energy conversion efficiency in partial load mode and self-thermal supported condition, decrease in heat loss, in particular, 400 W is strongly requested.

1. Introduction

Solid oxide fuel cells (SOFCs) are mainly consisted of metal oxide and operated at higher temperatures. Therefore, SOFCs realizes an internal reforming reaction on the anode, and this leads to a high energy conversion efficiency of the cell because it is not necessary to supply additional fuel for reforming and unused heat was effectively used [1,2]. Recently, field test of a combined heat and power generation (CHP) system using SOFCs for a residential application is started and it is expected that commercialization of SOFCs is approaching like polymer electrolyte fuel cell (PEFC) system for a CHP purpose [3–5]. However, there are still many issues to overcome for the requirement of residential CHP system. Since space of the household equipment is limited, SOFC has to achieve a small space for setting up system [6–8]. It is also requested to achieve a higher energy conversion efficiency than that of the current thermal power generation systems such as gas engines or polymer fuel cells. Furthermore SOFC have to follow the change in electric demands in house continuously and so, high energy conversion efficiency is also requested under partial load condition. Long service life is also requested for SOFC system because it is difficult for SOFCs to operate in a daily start and stop (DSS) mode [9]. This is because its high operating temperature requires large energy and long period for starting up. From these requirements, we designed SOFC module and system operating at intermediate temperature by using $LaGaO_3$ based oxide film which shows much higher oxide ion conductivity than that of Y_2O_3 stabilized ZrO_2, the most popularly used electrolyte for SOFCs [10–14]. Since power size of the currently developing SOFC CHP system is 1 kW class, some heat value is requested to add for keeping temperature of SOFC module [15,16]. Therefore it is necessary to design module with heat loss as small as possible from energy conversion efficiency, however, there is limited data reported for the power generating property in a load follow operation mode, especially thermal characteristics of the SOFC module under partial load condition. In this study, development of the SOFC module consisting of micro tubular cells which use $LaGaO_3$ electrolyte film was reported. Thermal self sustainability of the developed SOFC module was also designed based on the heat generation value in experimental section and the examined results based on the thermodynamic calculation was also reported.

* Corresponding author at: TOTO LTD, 2-8-1 Honson, Chigasaki-city, Kanagawa 253-8577, Japan. Tel.: +81 467 54 3538; fax: +81 467 54 1186.
E-mail address: naoki.watanabe@jp.toto.com (N. Watanabe).

0378-7753/$ – see front matter © 2011 Elsevier B.V. All rights reserved.
doi:10.1016/j.jpowsour.2011.10.071

Nomenclature

P	electrical power produced by cell stack [W]
V	stack voltage [V]
I	current [A]
n	number of electron
F	Faraday's constant [C m^{-1}]
U_f	fuel utilization [%]
N_{cell}	number of cell
ΔH_0	enthalpy flux [kJ mol^{-1}]
x_i	concentration of town gas composition
y_i	carbon molecular
$M_{13\,A}$	town gas flow volume [mol s^{-1}]
M_{steam}	steam flow volume [mol s^{-1}]
Q_{in}	inlet town gas heat value [W]
Q_{reform}	reformate endothermic heat value [W]
Q_{steam}	evaporate endothermic heat value [W]
Q_{cell}	cell stack heat generation rate [W]
Q_{comb}	combustion heat value [W]
q_{reform}	reaction heat flux of reforming reaction [kJ mol^{-1}]
q_{steam}	heat flux of evaporation [kJ mol^{-1}]
$q_{13\,A}$	town gas heat flux [kJ mol^{-1}]
η	electrical efficiency [%]

2. Experimental

2.1. Cell fabrication

A micro tubular single cell was prepared by using $NiO/(ZrO_2)_{0.9}(Y_2O_3)_{0.1}$ (NiO/YSZ) anode substrate, $NiO/(Ce_{0.9}Gd_{0.1})O_{1.95}$ (NiO/GDC10) interlayer, $La_{0.8}Sr_{0.2}Ga_{0.8}Mg_{0.2}O_{2.8}$ (LSGM) electrolyte, and $La_{0.6}Sr_{0.4}Co_{0.2}Fe_{0.8}O_3$ (LSCF) cathode. Cross section of the cell prepared is schematically shown in Fig. 1. The anode substrate tube of NiO/YSZ cermet was prepared by an extrusion molding technique. The anode interlayer NiO/GDC10 and the electrolyte LSGM were subsequently coated onto the anode substrate by a slurry coating method followed by co-firing in air. Finally, the cathode LSCF was coated onto the electrolyte layer by a slurry coating and fired. Fig. 2 shows a photograph of the micro tubular single cell prepared in this study. The single cell jointed to the current collector cap made by silver brazes metal [17,18].

2.2. Heat balance calculation

We calculated a heat value of each component and optimized the design of SOFC module. In order to consider a heat balance, it is requested to arrange the each component in according to the heat value into module for managing the heat energy effectively. Steam reforming and vaporization is both endothermic reactions. Since electrochemical oxidation in the cell stack and combustion

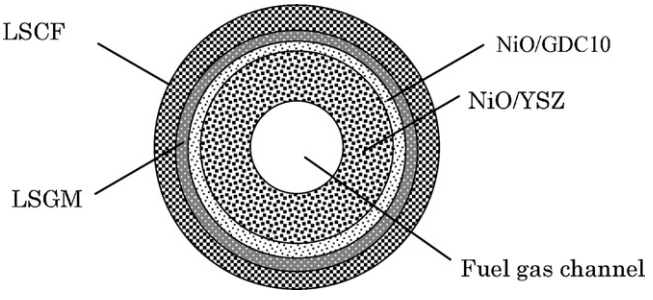

Fig. 1. Cell structure for single micro tubular single cell.

Table 1
Composition of city gas 13 A used for power generation measurement.

Composition	Volume%
CH_4	89.6%
C_2H_6	5.6%
C_3H_8	3.4%
C_4H_{10}	1.4%

are exothermic reaction, heat loss is considered a heat radiation from the module surface and heat energy carried by exhaust gas. We tried to calculate the heat value of each reaction under a condition of DC output power of 1000–100 W, fuel utilization U_f = 75%, Steam carbon ratio (S/C); 2.5, and town gas 13 A for fuel of which composition is shown Table 1 [19–21].

The output power of the cell stack can be expressed as the following equation (1).

$$P = V \times I \tag{1}$$

where P denotes the power. V and I are the cell stack voltage and the current density, respectively. The town gas flow volume, M, is expressed as follows:

$$M_{13\ A} = \frac{I}{nFU_f}\frac{N_{cell}}{A}, \quad A = \sum \frac{4n+m}{2}x_i \tag{2}$$

$$C_nH_m + 2nH_2O \rightarrow nCO_2 + \frac{4n+m}{2}H_2$$

where n, F, U_f, N_{cell} and x_i are number of electron, Faraday's constant, fuel utilization, number of cells and the concentration of town gas composition, respectively. We assumed constant A as 4.4959 that is corresponded to the sum of hydrogen molecule form of composition of each reforming reaction. Town gas heat flux and the inlet town gas heat value are expressed as follows:

$$q_{13\ A} = -\sum \Delta H_i^o \times x_i \tag{3}$$

$CH_4[g] + 2O_2[g] \rightarrow 2H_2O[g] + CO_2[g], \quad \Delta H^o_{CH_4} = -802.4$ (kJ mol^{-1})
$C_2H_6[g] + 3.5O_2[g] \rightarrow 3H_2O[g] + 2CO_2[g], \quad \Delta H^o_{C_2H_6} = -1427.8$ (kJ mol^{-1})
$C_3H_8[g] + 5O_2[g] \rightarrow 4H_2O[g] + 3CO_2[g], \quad \Delta H^o_{C_3H_8} = -2044.0$ (kJ mol^{-1})
$C_4H_{10}[g] + 6.5O_2[g] \rightarrow 5H_2O[g] + 4CO_2[g], \quad \Delta H^o_{C_4H_{10}} = -2648.5$ (kJ mol^{-1})

$$Q_{in} = M_{13\ A} \times q_{13\ A} \tag{4}$$

where ΔH_i^o is enthalpy flux of fuel. Reformate endothermic heat value and the reaction heat flux of reforming reaction are expressed as follows.

$$Q_{reform} = M_{13\ A} \times q_{reform} \tag{5}$$

$$q_{reform} = -\sum \Delta_r H^o x_i \tag{6}$$

$CH_4[g] + 2H_2O[g] \rightarrow CO_2[g] + 4H_2[g], \quad \Delta_r H^o = +165.0$ (kJ mol^{-1})
$C_2H_6[g] + 4H_2O[g] \rightarrow 2CO_2[g] + 7H_2[g], \quad \Delta_r H^o = +264.3$ (kJ mol^{-1})
$C_3H_8[g] + 6H_2O[g] \rightarrow 3CO_2[g] + 10H_2[g], \quad \Delta_r H^o = +374.9$ (kJ mol^{-1})
$C_4H_{10}[g] + 8H_2O[g] \rightarrow 4CO_2[g] + 13H_2[g], \quad \Delta_r H^o = +487.0$ (kJ mol^{-1})

where q_{reform} and $\Delta_r H^o$ are the reaction heat flux of reforming reaction and the enthalpy flux for each reaction. Steam flow volume and evaporate endothermic heat value are expressed as follows. For this calculation, we assume that S/C value is 2.5.

$$Q_{steam} = M_{steam} \times q_{steam} \tag{7}$$

$$M_{steam} = \sum 2.5M_{13\ A}x_iy_i \tag{8}$$

Fig. 2. Photographs of the prepared micro tubular cell.

where q_{steam} and y_i are the evaporate heat flux and carbon molecule in each hydrocarbon composition. Heat generation rate from the cell stack is expressed as follows.

$$Q_{cell} = (Q_{in} - Q_{reform})U_f - P \quad (9)$$

Here, heat value consumed in stack is expressed as $(Q_{in} - Q_{reform})U_f$. Heat generation rate from the cell stack was estimated by subtracting the output power from an inlet total heat energy. The combustion heat value of the unused fuel and air is also expressed as follows.

$$Q_{comb} = (Q_{in} - Q_{reform})(100 - U_f) \quad (10)$$

We defined that the heat loss, $Q_{heatloss,}$ is the sum of heat value generating in cell stack, combustion area and endothermic one from reformate and evaporator.

$$Q_{heatloss} = Q_{cell} + Q_{comb} + Q_{reform} + Q_{steam} \quad (11)$$

The calculation results will be compared with that of real operation measurement in following part.

2.3. Module design

SOFC module structure studied is shown in Fig. 3. SOFC module was consisted of the micro tubular cell stack, combustion area, fuel reformer, air heat exchanger and vaporizer in the metal jacket surrounded by inorganic heat insulators. The cell stack was consisted of about hundred cells arranged in all series connection and used metal current collector which was connected to the current collector cap. Combustion area works as burning off the unused fuel with air to support heat energy for cell module. Reformer should be arranged close to the cell stack and the combustion area as much as possible for effectively recovering a heat losing by radiation and the exhaust gas. Air heat exchanger should be designed for recovering the exhaust gas heat and heating air from room temperature to about 773 K because $Q_{heatloss}$ is kept to be positive. Vaporizer should also be designed for recovering the exhaust gas heat which is cooled by reformer and air heat exchanger. Insulator is arranged for preventing the heat radiation from the metal jacket. Insulator is made by SiO_2–TiO_2 based material in which thermal conductivity is about 0.020 W mK^{-1} and insulator thickness is 50 mm. Fig. 4 shows appearance of the SOFC module without insulators. The module dimension designed in this study is as follows; 460 mm width, 200 mm depth and 260 mm height.

2.4. Design of module system

Fig. 5 shows a system configuration which is designed for the SOFC module experimental set-up. Fuel used is a town gas 13 A and desulfurized before the module. Fuel pump supplies a town gas to the reformer and the air blower is installed in a fuel line for purging remained gas when the system is start up and shut down. Water pump supplies pure water to the vaporizer. Another air blower supplies air as an oxidant for the cathode of the cell. DC electric power generated by SOFC module is consumed by using an electrical load. Temperature is measured at each component during power generation measurement.

3. Results and discussion

Table 2 and Fig. 6 summarize the values used for heat parameter in this study. On these parameters, it was confirmed that $Q_{heatloss}$ is always a positive value under various power output conditions.

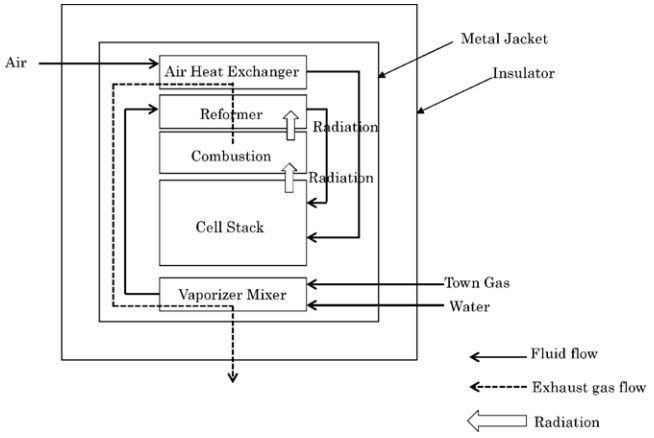

Fig. 3. Scheme of system design for 700 W class SOFC module.

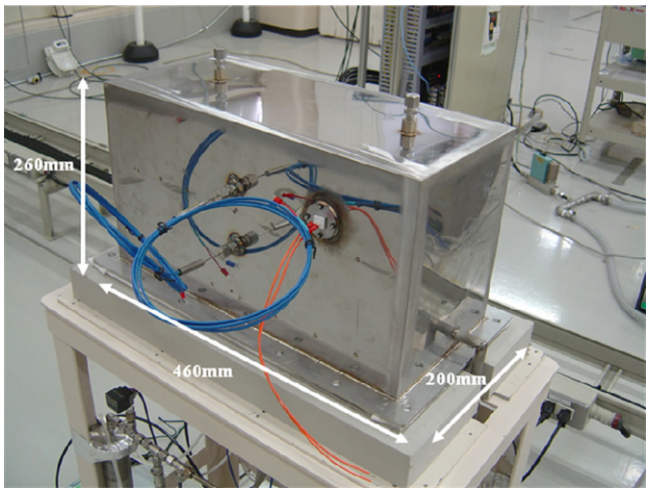

Fig. 4. Photographs of SOFC module prepared.

From the calculation results of module heat balance, we have to design that $Q_{heatloss}$ becomes a small value as much as possible by decreasing the heat loss by radiation from the module surface and that in exhaust gas for achieving the thermal self-supporting condition. In addition, it was found that $Q_{heatloss}$ is determined by efficiency of an air heat exchanger and thermal insulating property of insulator materials used in the cell stack.

It is noted that the heat generation rate Q_{cell} from the cell stack and a combustion heat value Q_{comb} did not increase monotonically with increasing SOFC output power. This could be explained by the non-monotonic performance of an electrode overpotential, namely, at small current density, change in current density is small in spite of change in power density as discussed below. Electrical efficiency decreased gradually with increasing SOFC output power. Electrical efficiency was calculated under constant U_f and temperature. Therefore, a calculated efficiency is higher than that of the real experimental one, especially in lower current density.

Fig. 7 shows the dependence of the consumed heat value inside stack and cell voltage as a function of current density. The heat value consumed in the stack is expressed as $(Q_{in} - Q_{reform})U_f$ and it increases monotonously as current density increases when U_f is kept constant (∵Eqs. (2)–(9)). On the other hand, cell voltage

Table 2
Heat value calculation at DC output power of 1000–100 W under a condition of fuel utilization U_f = 75%, steam carbon ratio (S/C); 2.5, and town gas 13 A for fuel.

Power [W]	Q_{cell} [W]	Q_{comb} [W]	Q_{reform} [W]	Q_{steam} [W]	$Q_{heatloss}$ [W]
1000	805.2	601.7	−403.2	−283.8	719.9
900	701.8	533.9	−357.8	−251.8	626.1
800	604.7	468.2	−313.7	−220.8	538.4
700	501.3	400.4	−268.3	−188.8	444.6
600	404.3	334.8	−224.3	−157.9	356.9
500	300.9	266.9	−178.9	−125.9	263.1
400	203.8	201.3	−134.9	−94.9	175.3
300	125.9	142.0	−95.1	−66.9	105.8
200	72.4	90.8	−60.8	−42.8	59.6
100	28.8	42.9	−28.8	−20.2	22.7

estimated by the calculation is not monotonically decreased with increasing current density because the potential drop by the activation overpotential is large at a low current density. Therefore, the heat generation rate Q_{cell} from the cell stack is dependent on the current density of the cell. The combustion heat value Q_{comb} is larger than that of the heat generation Q_{cell} from cell stack when the output power of SOFC module is smaller than 400 W. This is reasonably understood that the energy from SOFC power is smaller than that of the inlet heat value at lower current density because of large part of an inlet energy is used for keeping the cell temperature to operating one. Since Faraday's efficiency is high in this calculation condition, the heat generation rate Q_{cell} from the stack is found to be further smaller than the estimated one under small power density state, namely the partial load condition.

Fig. 8 shows the stack temperature and the open circuit voltage (OCV) of the SOFC stack as a function of time after start up. Stack temperature is achieved 973 K within about 100 min and the OCV also shows the theoretical value within the almost same period. Therefore, the developed SOFC module shows a reasonable short period for start up.

Fig. 9 shows the module output power and the stack temperature behavior after start up, when SOFC module is operating at about 800 W by controlling the current density and the feed rate of a town gas. Steam carbon ratio (S/C) is set to 2.5 under a reforming condition. Feed rate of pure water is also controlled in accordance with a town gas feed rate for keeping the steam/carbon (S/C) ratio same value. Stack temperature decreased gradually from 956 to 892 K and became stable since the SOFC module is operated at 956 K

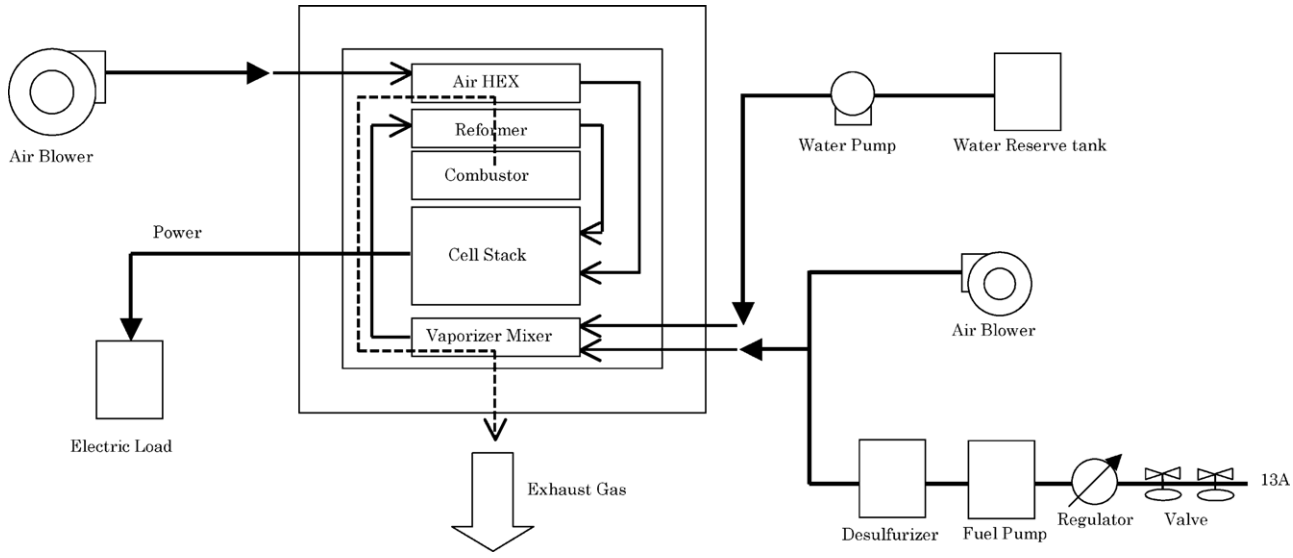

Fig. 5. Detail system diagram and flow of SOFC system designed.

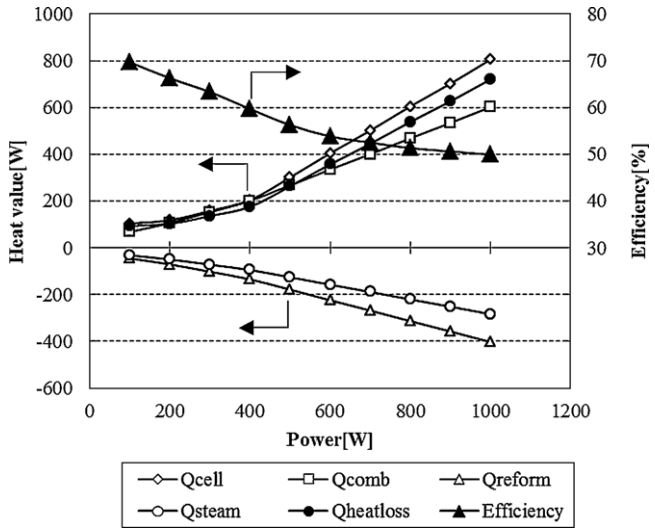

Fig. 6. Calculation results of each heat value as a function of SOFC output power.

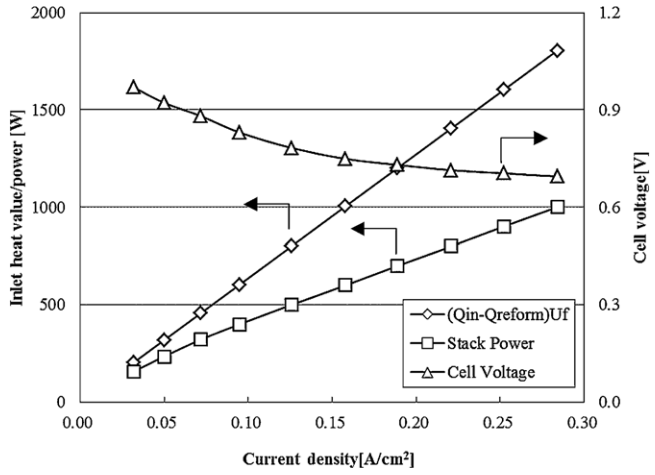

Fig. 7. Consumed heat value of inside stack and cell voltage as a function of current density.

under 70% fuel utilization. Thermal self supported state is defined that variations in a temperature change is smaller than 0.5 K h^{-1} under a constant current generation mode, which is corresponded to a period after 480 min from start up. In addition, the SOFC module power decreases gradually from 853 to 770 W at constant current

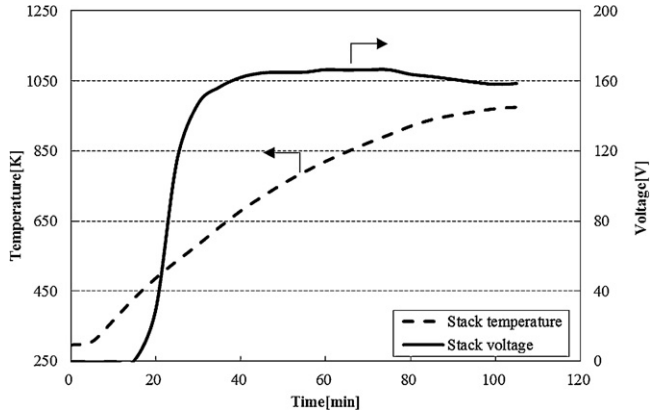

Fig. 8. Time dependence of stack temperature and OCV after startup.

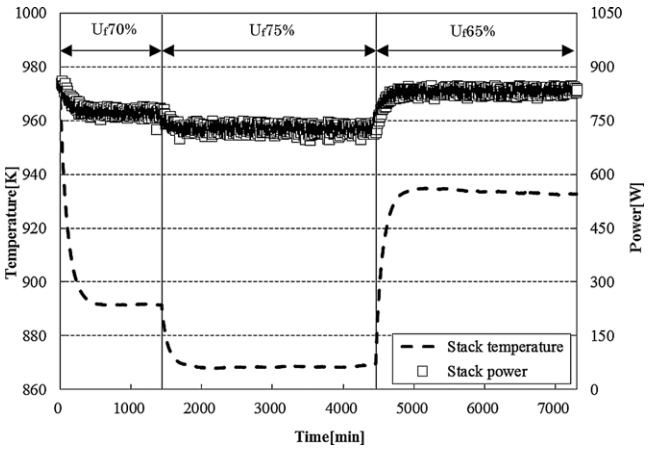

Fig. 9. Time dependence of module temperature and output power after changing fuel utilization.

density because of decreasing the stack voltage and then became stable in the power density.

Effects of operation condition on power generating property were further studied. Next examined operating condition is 75% fuel utilization that is achieved by decreasing town gas feed rate. In a similar manner with the previous case, stack temperature decreases gradually from 892 to 868 K and became stable. The SOFC module output power was about 729 W under this condition. Requested period to achieve the stable power generation is 282 min under a thermal self supported state. Next operating condition studied is 65% fuel utilization that was achieved by increase in a town gas feed rate. Stack temperature again increased gradually from 868 to 934 K and became stable. SOFC module power shown is about 824 W at this condition. It is requested 474 min before thermal self supported state achieved under the examined condition. It is evident that the total heat value can be controlled by a town gas feed rate, and the stack temperature was change depending on the fuel utilization or the output power. Change in those transient behaviors is slow, because SOFC module power is dependent on the stack temperature. By substituting these results into Eqs. (1)–(10), we can estimate the heat value during power generation in the developed module.

The module power dependency of each heat value is shown in Fig. 10. The stack terminal voltage and SOFC module power decreased because of increase in the Nernst loss at increased fuel

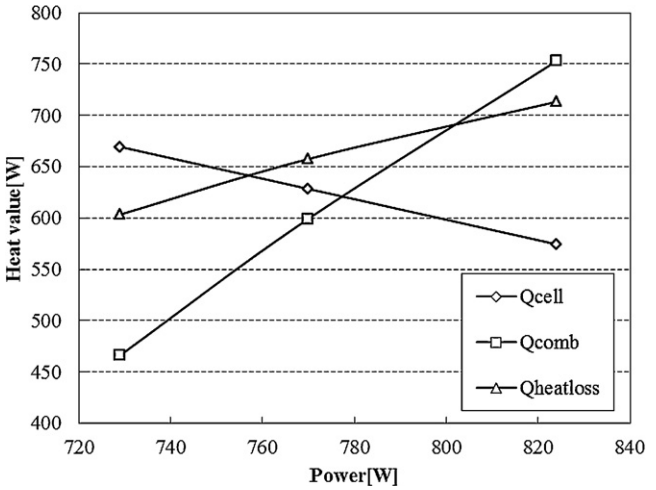

Fig. 10. Estimated cell stack heat generation rate, combustion heat value, and heat loss as a function of output power.

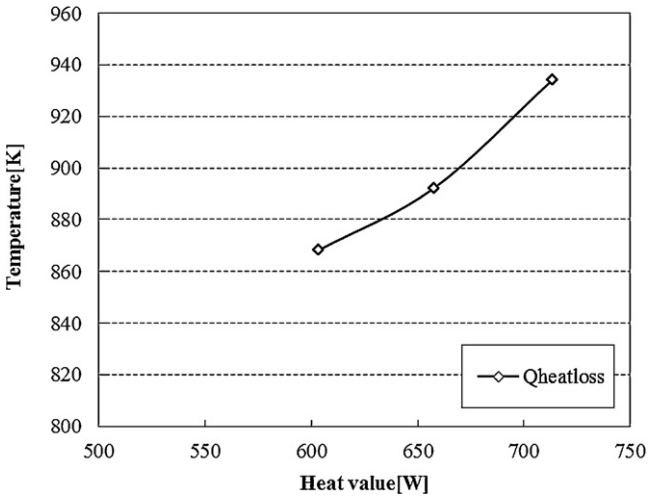

Fig. 11. Relationship between thermal self supported temperature and heat loss.

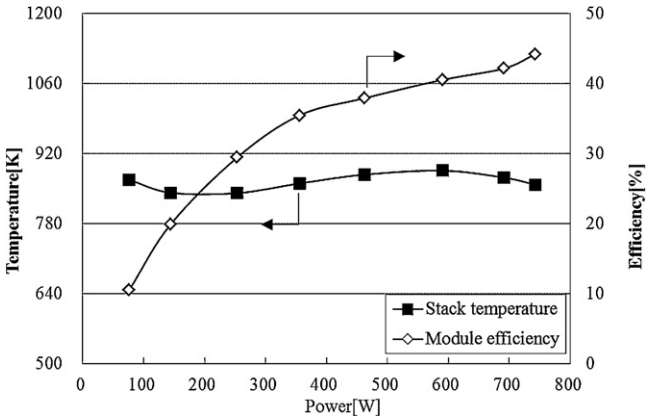

Fig. 12. SOFC module power dependence and energy conversion efficiency of the module as a function of output power.

utilization. Thus, the heat generation rate from the cell stack, Q_{cell}, increased with decreasing the cell stack voltage. On the other hand, the combustion heat value Q_{comb} is decreased by a raised fuel utilization and consequently $Q_{heatloss}$ decreased. Therefore, control of combustion heat value Q_{comb} is more effective for determining the stack temperature comparing with that of the cell stack heat generation rate Q_{cell}. Reason for decrease in stack temperature is a decreased combustion heat value Q_{comb} by raised fuel utilization.

Energy conversion efficiency for electrical power is expressed as follows.

$$\eta = 100\frac{P}{Q_{in}} \tag{12}$$

Energy conversion efficiency of 46, 46.3, and 47% LHV was estimated at the fuel utilization of U_f = 65%, 70%, 75%, respectively. Energy conversion efficiency can be improved by elevating fuel utilization. In fact, the highest efficiency of 49.5% LHV is achieved at U_f = 75% however, the energy conversion efficiency gradually decreased from 49.5 to 47% LHV with decreasing the output power density because of an insufficient heat flux for a thermal self supporting state. SOFC module is always requested to be thermal self supported even at a high fuel utilization value even under a partial load condition. However, under a partial load condition, heat generated from the cell stack became small and so operating temperature of the cell in thermal self support condition decreases resulting in the decreased energy conversion efficiency. In our previous study, the SOFC module power is significantly decreased by increasing the activation overpotential at stack temperature lower than 873 K. Therefore, we have to operate SOFC system of which stack temperature is higher than 873 K at any SOFC module output powers. Fig. 11 shows the heat loss value $Q_{heatloss}$ as a function of equilibrated temperature of the stack under a thermal self-standing condition. Stack temperature decreased with decreasing the heat loss value $Q_{heatloss}$ because of a high fuel utilization value. Therefore it is expected that stack temperature is difficult to be kept above 873 K as the SOFC module power is small at the constant fuel utilization.

We tried to operate the SOFC module by controlling the fuel utilization and air utilization in order to keep module operating temperature 873 K stably. Fig. 12 shows the module output power as a function of stack temperature and also the energy conversion efficiency. Stack temperature is kept approximately 873 K under the controlled utilization of fuel and air. This result means that stack temperature can be kept 863 ± 20 K under various electrical power demands in the house. The energy conversion efficiency decreases as the SOFC module power decreases. This is explained by the low fuel utilization for keeping cell temperature stable. Table 3 summarizes the SOFC module power, stack temperature, reformer temperature, reforming rate, and exhaust gas temperature under various operation conditions. Air utilization is controlled to keep a high value when the SOFC output power is smaller than 253 W in order to keep stack temperature. At the module structure in our SOFC system, the combustion area tends to be insufficient oxygen concentration when air flow rate was small. Exhaust gas temperature became minimum at 355 W of the SOFC module power. It is considered that the inlet heat energy is insufficient at this condition because of low stack temperature. Fig. 13 shows the heat value and temperature of SOFC stack as a function of the output power. Heat generation rate from the cell stack, Q_{cell}, decreased with decreasing the SOFC module power at the constant operation temperature. On the other hand, the combustion heat value, Q_{comb} tends to be high with decreasing the SOFC module power. In contrast, the reforming endothermic heat value Q_{reform} and the evaporation heat value Q_{steam} tend to be a small value as the SOFC module output power decreased. Heat loss by the surface heat radiation of the module can be suppressed by using the thermal insulator with a low thermal conductivity coefficient. On the other hand, heat loss value $Q_{heatloss}$ is achieved a value between 400 and 600 W and the corresponding stack temperature between 841 and 886 K under a thermal self

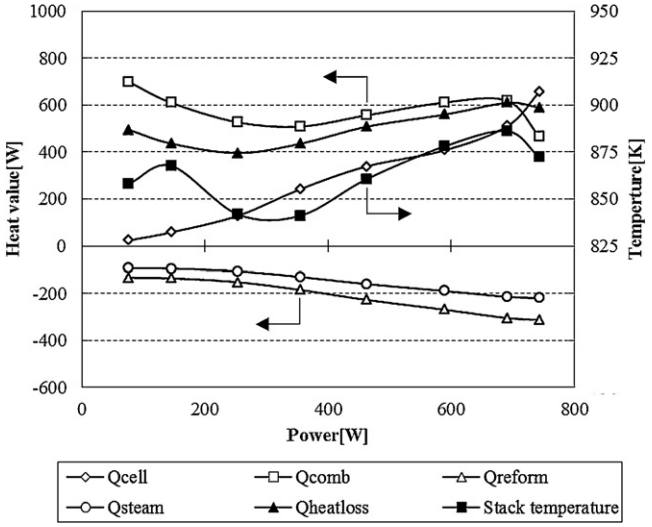

Fig. 13. Estimated each heat value and stack temperature as a function of output module power.

Table 3
Results of SOFC power, stack temperature and exhaust gas temperature at 7–0.5 A, U_f = 75–25%, U_a = 43–25%, S/C = 2.5.

Power [W]	Fuel utilization [%]	Air utilization [%]	Stack temperature [K]	Reformer temperature [K]	Reforming rate [%]	Exhaust gas temperature [K]
743	75	43	872.2	844.4	64.7%	566.2
691	66	40	886.2	858.4	69.5%	569.5
590	62	40	878.2	858.2	69.4%	543.2
462	59	40	860.6	852.6	67.5%	507.3
355	54	40	841.2	848.7	66.2%	456.0
253	42	35	841.9	861.8	70.6%	477.9
145	25	25	867.7	890.6	80.0%	490.3
76	25	25	858.2	889.2	79.6%	478.0

supported state. In this result, it is clear that the heat loss value $Q_{heatloss}$ is correlated with thermal self supported temperature.

4. Conclusion

SOFC module with 700 W class was designed and fabricated by using the micro tubular cells with LSGM film electrolyte and the fabricated module shows a thermal self supported state under various conditions as designed. The module heat balance was also estimated in this study, and it became clear that the cell stack heat generation rate Q_{cell} are strongly dependent on the SOFC output power. Since Faraday's efficiency is high in this calculation, the stack heat generation rate Q_{cell} is found to be small under a small SOFC output power, i.e. partial load condition. Because the heat value from the stack changes with a module output power, stack temperature is strongly related with the fuel utilization in a constant current mode. SOFC module can be thermally self supported within a limited temperature range, because of the limited fuel and air utilization from the requested heat value. The thermal self supported temperature is determined by the exhaust gas heat radiation and a heat radiation constant of the module surface. In this study, thermal property in the SOFC module was estimated for development of SOFC system that can achieve the high energy conversion efficiency under a partial load condition. For achieving the high energy conversion efficiency in a partial load mode and self thermal supported condition, decrease in heat loss strongly requests and it became clear that the utilization of fuel and air has limitation for thermal self support.

References

[1] H. Sumi, K. Ukai, Y. Mizutani, H. Mori, C.J. Wen, H. Takahashi, O. Yamamoto, Solid State Ionics 174 (1–4) (2004) 151–156.
[2] P.K. Cheekatamarla, C.M. Finnerty, Y. Du, J. Jiang, J. Dong, P.G. Dewald, C.R. Robinson, J. Power Sources 188 (2009) 521–526.
[3] O. Yamamoto, Electrochim. Acta 45 (15-16) (2000) 2423–2435.
[4] S.C. Singhal, Solid State Ionics 152-153 (2002) 405–410.
[5] M. Suzuki, T. Sogi, K. Higaki, T. Ono, N. Takahashi, K. Shimazu, T. Shigehisa, ECS Trans. 7 (2007) 27–30.
[6] J. Van herle, R. Ihringer, N.M. Sammes, G. Tompsett, K. Kendall, K. Yamada, C. Wen, T. Kawada, M. Ihara, J. Mizusaki, Solid State Ionics 132 (3) (2000) 333–342.
[7] M. Lockett, M.J.H. Simmons, K. Kendall, J. Power Sources 131 (1–2) (2004) 243–246.
[8] N.M. Sammes, Y. Du, R. Bove, J. Power Sources 145 (2) (2005) 428–434.
[9] H. Eto, T. Akbay, K. Hirata, M. Sato, T. Inagaki, F. Nishiwaki, ECS Trans 26 (1) (2010) 341–347.
[10] T. Ishihara, H. Furutani, T. Yamada, Y. Takita, Ionics 3 (1997) 209–213.
[11] S. Wang, M. Ando, T. Ishihara, Y. Takita, Solid State Ionics 174 (2004) 49–55.
[12] T. Ishihara, Bull. Chem. Soc. Jpn. Vol.79 (No.8) (2006) 1155–1166.
[13] T. Inagaki, F. Nishiwaki, S. Yamasaki, T. Akbay, K. Hosoi, J. Power Sources 181 (2) (2008) 274–280.
[14] A. Kawakami, S. Matsuoka, N. Watanabe, T. Saito, A. Ueno, T. Ishihara, N. Sakai, H. Yokokawa, Ceram. Eng. Sci. Proc. 27 (4) (2006) p3.
[15] Y. Mizutani, K. Hisada, K. Ukai, H. Sumi, M. Yokoyama, Y. Nakamura, O. Yamamoto, J. Alloys Compd. 408/412 (2006) 518–524.
[16] T.H. Lim, J.L. Park, S.B. Lee, S.J. Park, R.H. Song, D.R. Shin, Int. J. Hydrogen Energy 35 (2010) 9687–9692.
[17] N. Watanabe, A. Kawakami, T. Ooe, T. Ishihara, Trans. Jpn. Soc. Mech. Eng. B 76 (768) (2010) 104.
[18] N. Watanabe, A. Kawakami, T. Ooe, N. Reisen, T. Ishihara, Electrochemistry 78 (8) (2010) 671–677.
[19] M. Carl, N. Djilali, I.B. Morrison, J. Power Sources 195 (2010) 2283–2290.
[20] R.J. Braun, S.A. Klein, D.T. Reindl, J. Power Sources 158 (2009) 1290–1305.
[21] Z. Yu, J. Han, X. Cao, W. Chen, B. Zhang, Int. J. Hydrogen Energy 35 (2010) 2703–2707.